Piezoelectric nanocomposite sensors assembled using zinc oxide nanoparticles and poly(vinylidene fluoride)

John S. Dodds[1], Frederick N. Meyers[2] and Kenneth J. Loh[*1]

[1]*Department of Civil & Environmental Engineering, University of California, Davis, CA 95616, USA*
[2]*Department of Mechanical & Aerospace Engineering, University of California, Davis, CA 95616, USA*

Abstract. Structural health monitoring (SHM) is vital for detecting the onset of damage and for preventing catastrophic failure of civil infrastructure systems. In particular, piezoelectric transducers have the ability to excite and actively interrogate structures (e.g., using surface waves) while measuring their response for sensing and damage detection. In fact, piezoelectric transducers such as lead zirconate titanate (PZT) and poly(vinylidene fluoride) (PVDF) have been used for various laboratory/field tests and possess significant advantages as compared to visual inspection and vibration-based methods, to name a few. However, PZTs are inherently brittle, and PVDF films do not possess high piezoelectricity, thereby limiting each of these devices to certain specific applications. The objective of this study is to design, characterize, and validate piezoelectric nanocomposites consisting of zinc oxide (ZnO) nanoparticles assembled in a PVDF copolymer matrix for sensing and SHM applications. These films provide greater mechanical flexibility as compared to PZTs, yet possess enhanced piezoelectricity as compared to pristine PVDF copolymers. This study started with spin coating dispersed ZnO- and PVDF-TrFE-based solutions to fabricate the piezoelectric nanocomposites. The concentration of ZnO nanoparticles was varied from 0 to 20 *wt.*% (in 5 % increments) to determine their influence on bulk film piezoelectricity. Second, their electric polarization responses were obtained for quantifying thin film remnant polarization, which is directly correlated to piezoelectricity. Based on these results, the films were poled (at 50 MV-m^{-1}) to permanently align their electrical domains and to enhance their bulk film piezoelectricity. Then, a series of hammer impact tests were conducted, and the voltage generated by poled ZnO-based thin films was compared to commercially poled PVDF copolymer thin films. The hammer impact tests showed comparable results between the prototype and commercial samples, and increasing ZnO content provided enhanced piezoelectric performance. Lastly, the films were further validated for sensing using different energy levels of hammer impact, different distances between the impact locations and the film electrodes, and cantilever free vibration testing for dynamic strain sensing.

Keywords: nanocomposite; piezoelectricity; PVDF copolymer; SHM; strain sensing; zinc oxide nanoparticles

1. Introduction

Damage to civil infrastructure systems, such as fatigue, corrosion, impact, cracks, and extreme loading, pose a severe economic burden for society, lead to catastrophic structural failures, and

---

∗Corresponding author, Assistant Professor, E-mail: kjloh@ucdavis.edu

jeopardize public safety. A stark example of damage-induced structural failure is the collapse and falling of the Lakeview Drive Bridge onto Interstate-70 in South Strabane, Pennsylvania (2005). Post-failure analysis has found that cracks in the bridge superstructure allowed deicing salt and water to penetrate and corrode the reinforced-concrete structure's steel reinforcement bars, ultimately causing its collapse (Hasch 2005). In 2009, a ~4 cm (1.5 in) long structural crack has been identified in an eye-bar in the Interstate-80 San Francisco-Oakland Bay Bridge. The severity of damage and the need for immediate repairs has caused the Bay Bridge to be closed for five days, which subsequently impacted traffic, local businesses, and the surrounding communities (Reid 2010). More recently in 2010, a pipeline in San Bruno, California has ruptured due to outdated and poor welding, combined with a spike in pipeline pressure. (Barrager and North 2010). In fact, numerous other catastrophic events have occurred in the past, but most civil infrastructures today still rely on time-, labor-, and cost-intensive visual inspection practices for assessing structural performance and damage. In addition to visual inspection, some bridge inspections also use techniques such as chain-dragging, which is an inherently subjective technique (Ahlborn *et al.* 2010). These structural failures and their associated adverse societal impacts could have been prevented or mitigated if a robust structural health monitoring (SHM) system had been installed. Instrumented sensors as part of the SHM system would be able to provide quantitative measurements of structural performance or could even detect damage initiation and propagation.

As a result, significant research related to sensor development, damage detection algorithms, and structural health monitoring methodologies have been conducted over the last several decades (Doebling *et al.* 1998). For instance, accelerometers that are coupled with system identification techniques have been employed for quantifying global vibration modal changes to structural damage or environmental conditions. Accelerometers have also tracked the floor displacements of a test structure or a real building under seismic excitations (Ulusoy *et al.* 2011). However, the high installation and maintenance costs of these tethered accelerometers have motivated the development of wireless sensors. These wireless sensors do not depend on expensive coaxial cables for data communications and power delivery, are low cost, feature distributed computational capabilities, and are suitable for dense instrumentation (Lynch and Loh 2006). On the other hand, fiber optics and fiber Bragg grating (FBG) sensors have also been demonstrated for distributed structural sensing in laboratory and field applications (Kersey 1996). Regardless of the specific technology, the goal is to lessen society's dependency on schedule-based inspections and transition to a more reliable and efficient condition-based monitoring framework (Farrar and Worden 2007).

Unlike the aforementioned SHM technologies that are passive systems and only sense/measure structural response to ambient excitations (e.g., traffic and wind), piezoelectric transducers are active and by nature multifunctional such that they can be used for sensing as well as for actuation and energy harvesting. They can be commanded to actively interrogate structures and measure structural response on demand. For instance, lead zirconate titanate (PZT) piezo-ceramic transducers are commonly used for generating guided-waves in composite beams and structures for damage detection (Gu *et al.* 2011). The amount of structural damage can be quantified using techniques such as root-mean-square deviation (Park *et al.* 2003) or by measuring impedance and capacitance changes (Mascarenas *et al.* 2007). PZTs offer another unique advantage such that they are able to harvest energy from ambient structural vibrations for recharging batteries onboard wireless sensor nodes (Inman *et al.* 2007). While PZTs possess high piezoelectricity, they are brittle and can be challenging to use on complex structural surfaces or can act as defects when embedded in materials such as fiber-reinforced polymer composites. As a result, poly(vinyledene

fluoride) (PVDF) and its copolymer poly(vinylidene fluoride-trifluoroethylene) (PVDF-TrFE) have been sought as alternatives for active sensing and SHM. The piezoelectricity of PVDF has been first observed in 1969 by (Kawai 1969), and its polymeric nature allows it to conform to complex structural surfaces, cover large areas, and is relatively inexpensive. It has been shown that patterned PVDF can be used to actuate and receive guided waves in a manner similar to PZT transducers (Gao *et al*. 2006). In single films and in stacks, PVDF has also been used to harvest and store ambient power for a variety of applications (Beeby *et al*. 2006, Sodano *et al*. 2004). Unfortunately, its piezoelectric coefficients are on the order of 7 pC-N^{-1}, as compared to 160 pC-N^{-1} for PZT (Greeshma *et al.* 2009). PVDF-TrFE has comparable piezoelectricity to pristine PVDF but requires no stretching to enter its piezoelectric β-phase (i.e., a phase of crystal morphology where the film is more susceptible to poling) (Kang *et al.*, 2008). Nevertheless, the lower piezoelectricity of PVDF and PVDF-TrFE has limited their applications for SHM despite their favorable mechanical flexibility and conformability to structural surfaces.

Because of the individual drawbacks of piezoelectric ceramics and polymer, the research community has progressed towards the development of novel piezoelectric materials that encompasses the high piezoelectricity of piezo-ceramics and the mechanical attributes of piezo-polymers. Some examples of piezoelectric composites include ones fabricated with PZT, PVDF, $Pb(Mg_{1/3}Nb_{2/3})O_3$-PbTiO$_3$ (PMN-PT), and aluminum nitride, among many others (Beeby *et al.* 2006, La Saponara *et al*. 2011). In addition, advancements in nanotechnology have motivated the development of nanocomposites featuring piezoelectric zinc oxide (ZnO)-based nanomaterials (e.g., nanowires, nanobelts, nanosprings, sheets, and nanotubes) (Tu and Hu 2006, Wang 2004).

The piezoelectricity of ZnO-based nanocomposites has been demonstrated and used as a dynamic strain sensor and power harvester (Loh and Chang 2010, Xu *et al*. 2010). ZnO has also been incorporated with PVDF, and the nanocomposite's piezoelectric performance has been characterized using impedance analysis, ultraviolet-visible analysis, and X-ray diffraction (Devi and Ramachandran 2011, Gaur and Indolia 2011). Fabrication extends beyond solvent casting, and faster techniques such as electro-spinning ZnO onto PVDF mats or dipping ZnO mats into PVDF solutions have also been achieved (Öğüt *et al*. 2007). More recently, spin coated PVDF-TrFE/ZnO thin films have also been studied and their remnant polarization characterized as a function of ZnO concentrations (Dodds *et al.* 2012). However, prior to their use for SHM, more detailed analysis of their sensing performance in laboratory settings is needed.

The goal of this study is to characterize the piezoelectric and sensing performance of spin coated PVDF-TrFE/ZnO thin films and how their piezoelectricity varies with ZnO nanoparticle concentrations. The outline of this paper is as follows. First, the fabrication procedure to spin coat the nanocomposites and the high-voltage poling process for enhancing piezoelectricity are discussed. A total of five unique sample sets of varying ZnO concentrations (i.e., ranging from 0 to 20 *wt.*% in 5 *wt.*% increments) have been fabricated. Second, thin film remnant polarization has been quantified by subjecting films to high-voltage alternating current (AC) excitations for obtaining their electric polarization-to-electric field hysteresis response. Then, their sensing performance and piezoelectricity differences due to different ZnO concentrations have been investigated using voltage time history results from hammer impact tests. The prototype PVDF-TrFE/ZnO thin films' performances have also been compared to results obtained using commercially poled PVDF-TrFE specimens. Free vibration tests, where samples are mounted onto a flexible cantilever beam and excited, have been used as the validation for dynamic strain sensing.

2. Experimental details

2.1 Raw materials

Raw materials such as zinc oxide nanoparticles (spherical, 20 nm diameter) were obtained from Nano Amor, and PVDF-TrFE (65:35) powder was obtained from Measurement Specialties. Commercial poled PVDF-TrFE thin films (28 μm thick) were also purchased from Measurement Specialties and were used for comparison purposes. The solvent used in this study, methyl ethyl ketone (MEK), along with disposable laboratory supplies, glass microscope slide substrates, and other materials were all from Fisher Scientific. Electrode components such as conductive copper tape and colloidal silver paste were purchased from Ted Pella. Finally, discrete circuit elements (such as resistors and capacitors) and electronic components used for assembling the Sawyer-Tower and poling circuits were from Digi-Key.

2.2 Thin film fabrication

An overview of the film fabrication procedure using spin coating is schematically illustrated in Fig. 1 and is described in greater detail in this section. First, PVDF-TrFE copolymer was dissolved in the polar solvent MEK by stirring at 50°C (Gaur and Indolia, 2011). Secondly, ZnO nanoparticles were added to the PVDF-TrFE solution at appropriate proportions so as to obtain 0 to 20 *wt.*% PVDF-TrFE/ZnO solutions. A total of five unique sets of solutions were prepared by varying ZnO concentrations in 5 *wt.*% increments. Each PVDF-TrFE/ZnO solution was prepared in 20 mL batches and stored in a scintillation vials, which was then subjected to bath ultrasonication (135 W, 42 kHz) to disperse the nanoparticles. Sonication was performed for 180 min or until when adequate dispersion was visually observed. Without ultrasonication, the ZnO nanoparticles agglomerated and were unsuitable for film fabrication. One would not be able to take advantage of the unique properties and high piezoelectricity offered by ZnO nanoparticles if they were not evenly dispersed in the film.
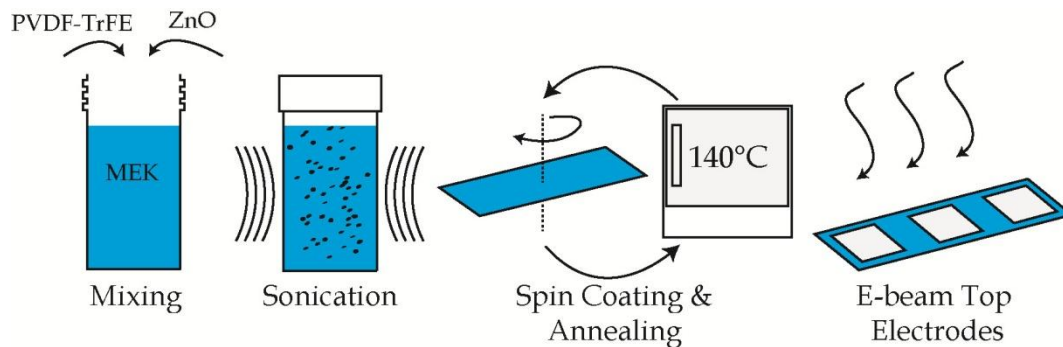

Fig. 1 To fabricate PVDF-TrFE/ZnO thin films, the solution has been bath ultrasonicated to completely disperse all particles. Next, the dispersed solutions have been spin coated to form thin films onto electrode-coated substrates. After annealing, e-beam deposition has been used to deposit the top aluminum electrodes

The next step in the fabrication process was spin coating thin films using the dispersed ZnO- and PVDF-TrFE-based solutions. Prior to spin coating, an electron-beam (e-beam) evaporator was used to deposit a thin (~150 nm) aluminum (Al) electrode onto glass microscope slides or flexible polymer sheets (0.01 mm thick). The Al-coated slide was then mounted in a Laurell spin processor where spin coating was performed to deposit layers of PVDF-TrFE solution. Spinning was performed first at 400 rpm for 5 s, then directly followed by spinning at 3,000 rpm for 30 s. This two-step procedure was adopted because the first step spread the solution so that it covered the whole slide, while the latter step spun the solution to the desired thickness of 3 to 4 μm (i.e., when 150 mg-ml^{-1} of the PVDF-TrFE copolymer in MEK was employed; a higher concentration produced a thicker film). Upon spin coating, the slide was annealed at 140°C for 2 min before additional layers were spin coated for obtaining thicker films. Once the desired film thickness was achieved, the film underwent a final annealing step at 140°C for 2 h; this final annealing step was important for safeguarding against film breakdown (where the film shorts due to a high electric field applied across it) during high-voltage poling. Finally, e-beam deposition was employed (in conjunction with a plastic mask) for depositing three rectangular Al electrodes (each approximately 1x1 cm^2) onto the film surface. Films between each electrode were removed by selectively dissolving them using MEK or by mechanical etching using a razor blade. Thus, this fabrication procedure yielded three PVDF-TrFE/ZnO thin film specimens for each spin coated thin film.

2.3 Remnant polarization hysteresis tests

The piezoelectric potential of PVDF-TrFE/ZnO thin films was characterized by measuring their electric displacement or polarization (*D*) in response to a high AC electric field following the procedure previously adopted by (Dodds *et al.* 2012). A 10 Hz AC waveform was applied across the thickness of the film using an Agilent 33210A arbitrary waveform generator and an Ultravolt 5HVA24 high voltage module. The maximum applied electric field (where $E=V/t$, *V* is the applied voltage, and *t* is film thickness) was set to 50 MV-m^{-1} in this study, although it was found by (Dodds*, et al.* 2012) that spin coated films of this type can possibly withstand electric fields as high as ~110 MV-m^{-1} before film breakdown. A Dektak IIA profilometer was used to measure the thickness of each film, and the voltage required to achieve 50 MV-m^{-1} was calculated for each specimen. The applied electric field and the corresponding film polarization were measured using a Sawyer-Tower circuit and an Agilent MSO8104A mixed-signal oscilloscope. The resulting *D-E* hysteresis responses of the PVDF-TrFE/ZnO films were used for determining their remnant polarizations, which are indicative of the piezoelectric potential of the bulk nanocomposite. It should also be mentioned that the films can be reused even after breakdown, repeated electrical testing, and fatigue by re-annealing (Section 2.2) and re-poling them (Section 2.4) (Zhang *et al.* 2005).

2.4 Poling

The films' piezoelectric properties were enhanced by high electric field poling, following the experimental setup as illustrated in Fig. 2. After spin coating the PVDF-TrFE/ZnO thin films, their electrical domains were randomly oriented, and bulk film piezoelectricity was low. However, the application of a high voltage direct current (DC) field would align the majority of the electrical

domains in the same direction, thereby enhancing piezoelectricity (Fig. 2(c)) (McKinney *et al*. 1980). For this experiment, PVDF-TrFE/ZnO thin films were immersed in silicone oil and heated to 75℃ (Bharti *et al*. 1997, Hilczer *et al*. 2000). Then, the Ultravolt amplifier was again employed for amplifying the DC voltage signal, which was generated by an Agilent E3642A DC power supply, up to 50 MV-m^{-1}. Each film was poled by applying the high electric field across its thickness, changed appropriately as per the film's thickness in order to maintain a voltage of 50 MV-m^{-1}. The magnitude of the DC electric field was chosen based on other work involving poling of piezoelectric polymers (Hilczer *et al*. 2000), and it was also found that high concentrations (15 and 20 *wt*.% ZnO) of PVDF-TrFE/ZnO thin films broke down due to higher applied electric fields (Dodds *et al*. 2012). During poling, the oscilloscope and a Sawyer-Tower circuit were used to monitor the voltage across each specimen. The film temperature, maintained at 75℃ during poling, was subsequently cooled to room temperature before removal of the applied electric field to ensure that the aligned domains were locked in their poled position (Arlt and Wegener 2010). Lastly, film capacitance was measured before and after poling to ensure that the measurements remained the same and that the films remained intact and had not electrically broken down.
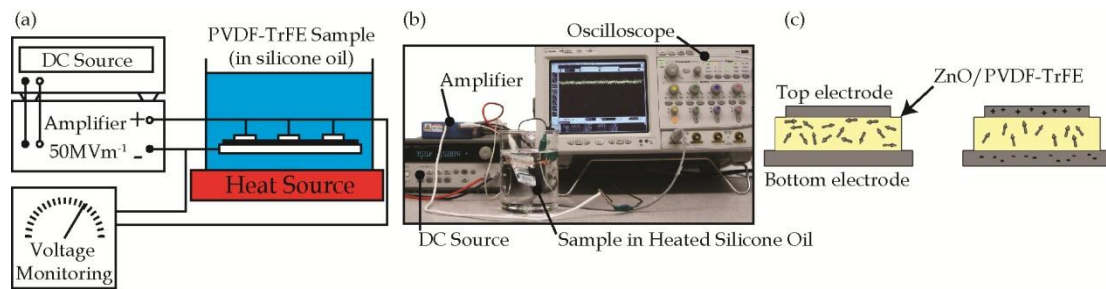

Fig. 2 (a) Poling has been achieved by applying an amplified DC voltage across a film specimen, (b) A picture of the actual experimental setup is also shown, and (c) after poling, the dipoles or electrical domains become aligned in the direction of the applied electric field

2.5 Hammer impact testing

Validation of PVDF-TrFE/ZnO thin film piezoelectricity and comparison of sensing performances for films with varying concentrations of nanoparticles were conducted using hammer impact tests as shown in Fig. 3. Spin coating based on the procedure described in Section 2.2 was followed for depositing a PVDF-TrFE/ZnO thin film onto the surface of one end of a glass microscope slide substrate. Then, a commercial poled PVDF-TrFE thin film was mounted onto the surface of the opposite end of the substrate using a cyanoacrylate adhesive. E-beam evaporation was again employed for depositing Al-electrodes onto both PVDF-based films. The size of the films and deposited electrodes were controlled to be approximately the same. The PVDF-TrFE/ZnO thin film was electrically poled at 50 MV-m^{-1} as per Section 2.4. Then, the entire slide and films were mounted in a customized hammer impact test apparatus and secured in the sample holder as shown in Fig. 3.

The hammer was dropped such that impact occurred halfway between the two films. Different drop heights were also used to test sensitivity to the energy of impact. In this configuration,

vibrations induced in the center of the slide propagated to either end and arrived at the sensors with the same phase and magnitudes. The voltage time history responses of both films were simultaneously measured using a multi-channel Agilent MSO8104A oscilloscope. Since the films were piezoelectric, no input power was supplied and only the films' voltage responses were recorded. Similarly, the magnitude of voltage generated was directly correlated to bulk film piezoelectricity, where higher generated voltages suggested greater thin film piezoelectric coefficients.

Specifically, the sensitivity of the film with regard to different impact energies was assessed. Different energies were obtained by using the impact device to drop the hammer from various angles. Impact energy was calculated using potential energy of the hammer above the point of impact ($PE=mgh$, where m is the mass of the hammer, h is the vertical drop height, and g is gravity). The maximum impact angle was 12° to prevent cracking the glass slide, and the minimum impact angle was 2.5°. Also investigated was the effect that impact distance had on the maximum voltage response. The sample holder was moved such that the hammer impacted the substrate at a location ranging from 10 to 25 mm away from the edge of the sample electrode (in increments of 2.5 mm). This test was carried out by releasing the hammer at 2.5° above the horizontal. More expansive distance testing was limited by the size of the hammer testing device and substrate mount.
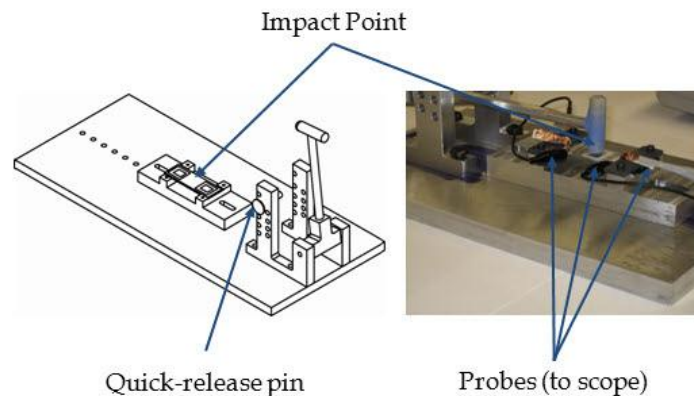

Fig. 3 This schematic and picture of the hammer impact testing apparatus illustrate the impact location of the hammer and the electrical probing setup

2.6 Free vibration testing

Free vibration testing was performed with the films deposited onto flexible poly(ethylene terephthalate) (PET) sheets, as was described in Section 2.2. These samples were then affixed onto poly(vinyl chloride) (PVC) thin plate specimens (30x7x0.3 cm^3) using a cyanoacrylate adhesive. A metal-foil strain gage (Tokyo Sokki Kenkyujo) was also attached to the PVC cantilevered beam and adjacent to the PVDF-TrFE/ZnO films. As shown in Fig. 4, each PVC beam with the attached thin films and strain gage was clamped to a lab bench at one end, and an initial excitation was

provided to initiate free vibration (i.e., via an initial displacement). Voltage was measured across three PVDF-TrFE/ZnO specimens simultaneously using an oscilloscope, with the fourth channel of the oscilloscope employed for measuring strain gage output. Strain was measured by connecting the strain gage to a Wheatstone bridge and amplification circuitry. In this manner, voltage output of the piezoelectric samples could be directly and simultaneously compared to measured strains.
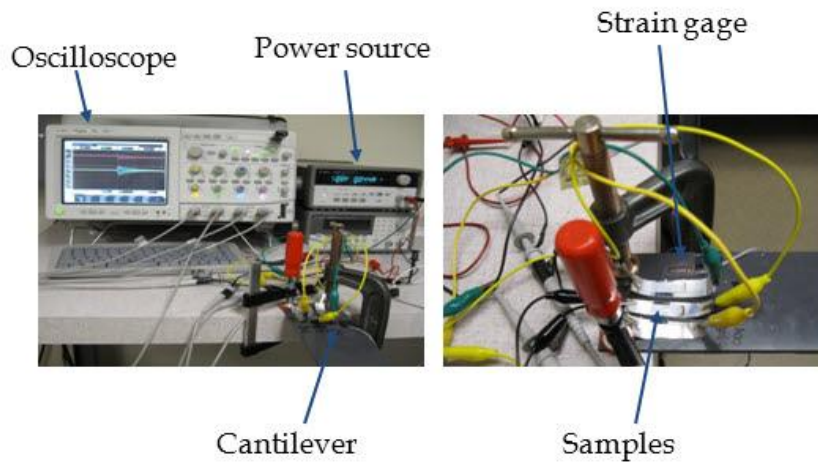

Fig. 4 The experimental setup for the free-vibration test is shown. The image on the left shows the use of an Agilent oscilloscope for data acquisition, and the image on the right shows the simultaneous querying of three PVDF-TrFE/ZnO thin films (along with the strain gage adjacent to the film specimens)

3. Results and discussions

3.1 Ferroelectric hysteresis characterization

As mentioned in Section 2.3, PVDF-TrFE/ZnO thin films of different concentrations have been subjected to high voltage AC signals (up to 50 MV-m^{-1}) for characterizing each of their electric polarization-to-electric field *(D-E)* hysteresis response. Representative *D-E* hysteresis loops corresponding to each ZnO concentration are plotted and overlaid in Fig. 5. First, from Fig. 5, it can be seen that the hysteresis loops transitions from an approximately linear line for 0 *wt.%* ZnO-based thin films to larger hysteresis loops with increasing ZnO concentrations. The linearity indicates that no domain shifting is occurring at that poling voltage for the 0 *wt.%* ZnO film; its piezoelectric properties are not being improved by poling. More hysteresis in films with higher ZnO concentrations indicates higher piezoelectricity, as can be seen in Fig. 5.

Secondly, remnant polarization, which is an important indicator of bulk film piezoelectricity, is determined by calculating the intersection of the *D-E* hysteresis loop with the electric displacement axis. In other words, remnant polarization is the electric displacement when there is no electric

field applied across the material. Theoretically, remnant polarization indicates the distance between the center of mass of the positive and the negative charges in the material or an equivalent dipole moment at zero electric field. The larger this charge separation, the more charge will be generated across the material from the same amount of force (Defay 2011). It has been shown by (McKinney *et al.* 1980) that there is a linear relationship between remnant polarization and a material's piezoelectricity.

The remnant polarization for representative films, as calculated from Fig. 5, increases from approximately 0 for 0 *wt.*% ZnO up to 0.0098 C-m^{-2} for 20 *wt.*% ZnO-based films. Films with 5, 10, and 15 *wt.*% ZnO show average remnant polarizations of 0.0008, 0.0036, and 0.0078 C-m^{-2}, respectively. It is clear that remnant polarization, and similarly bulk film piezoelectricity, increases in tandem with greater concentrations of ZnO nanoparticles embedded in the PVDF-TrFE polymer matrix. Because these thin films have been poled under the same conditions (i.e., same voltage, frequency, and ambient conditions), the change in remnant polarization is due to the increasing ZnO content. These results suggest that in addition to aligning the PVDF-TrFE electrical domains in the polymer matrix (which is the same for all samples), bulk film piezoelectricity increases with increasing ZnO concentrations because more piezoelectric ZnO nanoparticles participate and are also being aligned to the applied electric field. These trends are similar to *D-E* hysteresis loops obtained when testing PVDF-TrFE/ZnO thin films using different excitation voltages (Dodds *et al.* 2012).
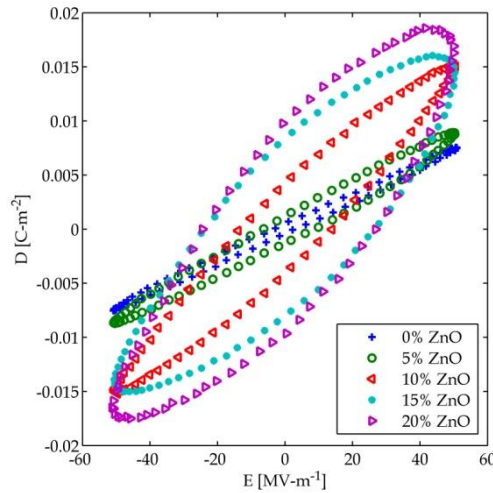

Fig. 5 Representative *D-E* hysteresis loops for films of different ZnO concentrations have been obtained after ferroelectric characterization. The applied electric field is 50 MV-m^{-1}. The remnant polarization increases with greater ZnO weight content

3.2 Hammer impact sensing

The hammer impact test, as have been described in Section 2.5, illustrates piezoelectricity in the prototype thin films and indicates film sensitivity depending on ZnO concentrations. For the

initial test, in order to provide the same impact energy to every sample, the hammer is released from 6° relative to the film. When the hammer strikes the substrate, guided waves propagate toward the thin film sensor and the commercial PVDF-TrFE film. The voltage responses for both films have been measured across their thicknesses and have been recorded by the oscilloscope. To avoid problems associated with bouncing, the oscilloscope is triggered to only measure the initial voltage response of the film. As can be seen from Fig. 6, increasing ZnO content of a film provides increased voltage sensitivity to elastic waves in the substrate. This is consistent with the increase in remnant polarization as have been demonstrated with the hysteretic characterization of this material (Section 3.1). A higher initial voltage peak response indicates that a film is more sensitive to surface waves and hence more piezoelectric. From Fig. 6, it can also be observed that the decay of the voltage response is proportionally consistent across different percentages of ZnO.
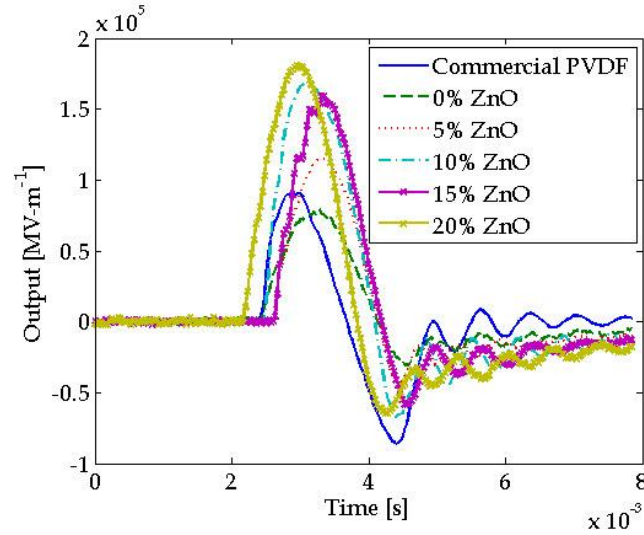

Fig. 6 The voltage time history responses of representative thin films with different ZnO concentrations subjected to hammer impact testing are overlaid. The results suggest that increasing ZnO concentration increases the film's sensitivity to hammer impact

Fig. 7 plots the average and standard error of the mean of the relative maximum voltage response for films of different ZnO concentrations. The relative maximum voltage ($V_{R,Max}$) is calculated by computing the ZnO-based film's maximum voltage ($V_{Max-ZnO}$) divided by the maximum voltage generated by the corresponding commercial PVDF-TrFE specimen mounted on the same slide ($V_{Max-PVDF}$). The calculation is also shown in Eq. (1)

$$V_{R,Max} = V_{Max-ZnO} \Big/ V_{Max-PVDF} \tag{1}$$

Eq. (1) uses the commercial PVDF as a reference so that any experimental errors such as variations in impact between trials or between films are adequately accounted for. Thus, according to Eq. (1), $V_{R,Max}$ should theoretically be equal to 1 for tests conducted on the prototype 0 *wt.%*

PVDF-TrFE/ZnO films if one assumes that they are poled in the same direction and manner as the commercial PVDF-TrFE specimens. In this case, it can be seen that the average $V_{R,Max}$ for 0 *wt.%* PVDF-TrFE/ZnO films is ~1.3 (Fig. 7), thereby suggesting that the films fabricated for this study are more sensitive than their commercial counterpart. While it is unlikely that the prototype films are poled to possess higher piezoelectricity than the commercial specimens, it is more likely that the commercial films have been poled in a slightly different manner; nevertheless, the data in Fig. 7 corresponding to the 0% case serves as the baseline for comparison.

Next, it can also be observed from Fig. 7 that the average relative maximum voltage increases in tandem with increasing ZnO concentrations. This result suggests that increasing ZnO content enhances the piezoelectricity of PVDF-TrFE thin films, and greater ZnO content provides greater enhancement. It appears from the result shown in Fig. 7 that the enhancement has plateaued after the addition of 10 *wt.%* ZnO, although mild improvements in piezoelectricity are observed with continued increasing ZnO content; however, additional testing will need to confirm this. Thus, based on the results shown in Figs. 6 and 7, one can conclude that given the same amount of mechanical excitation, poled PVDF-TrFE films with more embedded ZnO nanoparticles will be able to produce a higher voltage output, thereby making this film more viable for sensing and SHM applications.
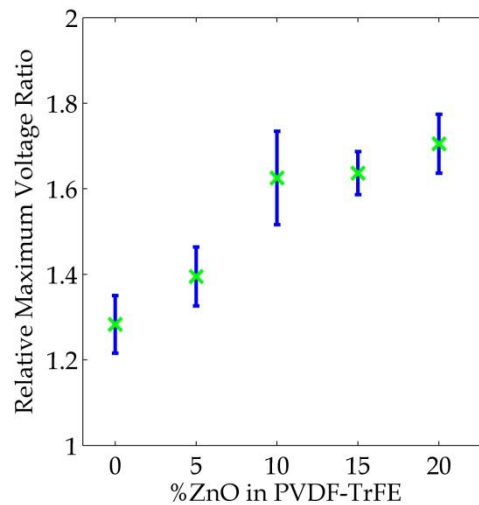

Fig. 7 The results of hammer impact testing are summarized, and the average relative maximum voltage and the corresponding standard error of the mean are plotted as a function of ZnO concentrations

As mentioned before in Section 2.5, film sensitivity to hammer impact energy has also been investigated. As expected, higher impact energies correspond linearly with higher peak voltage responses, as can be seen in Fig. 8. Since piezoelectricity is a linear phenomenon, this linear correlation with energy increase is appropriate and expected. As before, increasing ZnO concentrations in the film gives increasing peak voltage responses.

Piezoelectric sensitivity to impact distance from the film has also been explored. Fig. 9 demonstrates an example of the observed phenomenon. For a film with 20 *wt.%* ZnO nanoparticles,

an inverse relationship is observed between increasing distances between the impact location and the film electrode versus the measured voltage response. This result suggests that there are some limits as to the maximum distance from which impact can still be detected. Further testing will be explored in order to determine the maximum distance at which these films can sense impact on a substrate and in order to best optimize them for SHM.
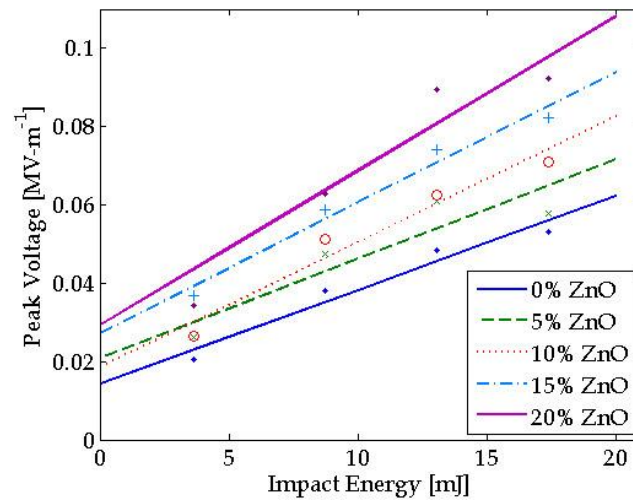

Fig. 8 The peak voltages (normalized by film thickness) generated by different energy impacts are plotted. In addition, representative results are shown for each thin film sample set. Increasing impact energy increases the measured peak voltage response
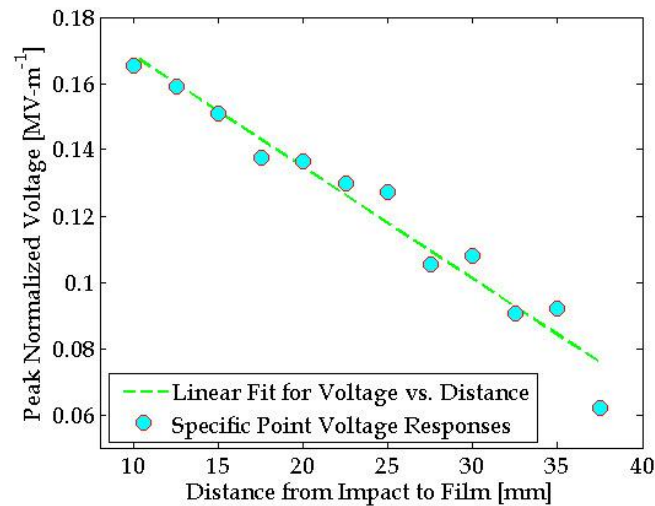

Fig. 9 Piezoelectric distance tests have been conducted, and the results show that the voltage response of the thin film decreases with increasing distance (i.e., between the film and location of impact). The result for a 20 wt.% PVDF-TrFE/ZnO thin film is shown

3.3 Dynamic strain sensing validation

Free vibration validation tests have also been performed according to the procedure outlined in Section 2.6 for dynamic strain sensing validation. Here, PVDF-TrFE/ZnO specimens have been affixed onto PVC cantilever beams. Voltage generated across the films during free vibration has been directly compared with measured strains. Dynamic strain ($\varepsilon_D = d\varepsilon/dt$) rather than strain has been considered, because a piezoelectric material supplies a voltage due to a change in instantaneous strain, rather than due to a constant level of applied strain. Fig. 10 gives two examples of thin film free vibration generated voltage responses overlaid with the dynamic strain time history as determined from strain gage measurements. The top plot of Fig. 10 shows the response for a typical 0 *wt.*% ZnO film, whereas the bottom plot shows the response for a typical 10 *wt.*% PVDF-TrFE/ZnO film. It should be mentioned that the raw data have been down-sampled by 50 in order to produce the plots shown in Fig. 10. For both graphs, it can be seen that the dynamic strain and the voltage generated have the same phase and frequency and change in tandem with one another, thereby confirming the piezoelectric relationship between the two. The film with proportionally more ZnO nanoparticles is more sensitive, which is as expected from previous results.
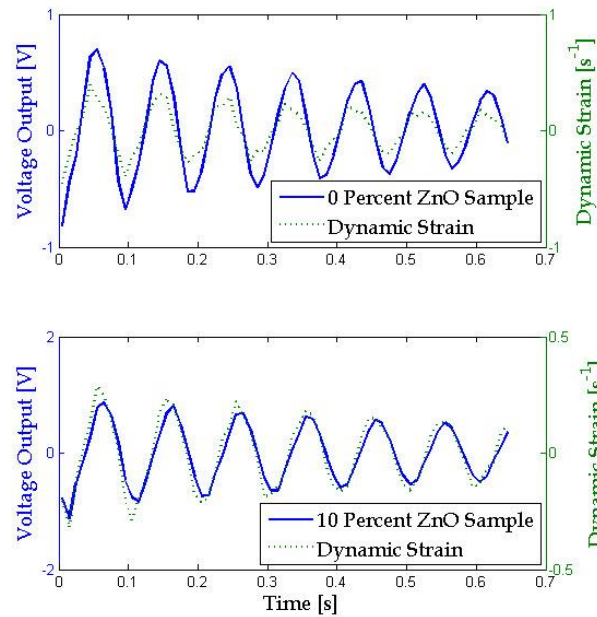

Fig. 10 Free vibration testing has been conducted, and two representative thin film voltage time history responses are plotted and overlaid with the dynamic strain time histories. The top plot shows the response for a representative spin coated 0 *wt.*% PVDF-TrFE/ZnO thin film, whereas the bottom plot is for one with 10 *wt.*% ZnO

Fig. 11 shows a more direct relationship between thin film piezoelectric response and dynamic strain; here, only the first few cycles of vibration are plotted for clarity purposes. As expected, the relationship between generated voltages and applied dynamic strain is linear without offset. Similar to Fig. 10, the top graph of Fig. 11 presents the results from the same 0 *wt.*% ZnO specimen, and the bottom graph shows results from the same 10 *wt.*% ZnO specimen. Linear least-squares best-fit lines have also been computed and overlaid on top of the data as shown in Fig. 11. The correlation coefficients have been calculated to be 0.959 and 0.966 for the 0 *wt.*% and 20 *wt.*% PVDF-TrFE/ZnO thin films, respectively, thereby demonstrating strong correlation between the two parameters. It should be mentioned that other specimens tested have also exhibited similar types of responses, and only two representative results are shown in Fig. 11. In addition to the observed positive correlation, the slopes of these least-squares best-fit lines are equivalent to the dynamic strain sensitivity (S_D) of these films and can be calculated using Eq. (2)

$$S_D = \frac{(\Delta V/\Delta t)}{(\Delta \varepsilon/\Delta t)} \tag{2}$$

where ΔV is the change in voltage over a time step Δt, and $\Delta \varepsilon$ is the change in strain over a time step Δt. As expected, the 0 *wt.*% ZnO film has a sensitivity of 1.93 and is lower than the dynamic strain sensitivity for the 10 *wt.*% ZnO film, which is 3.24 in this case. These results and trends are consistent with the ferroelectric characterization and hammer sensitivity test results as discussed in Sections 3.1 and 3.2, respectively.
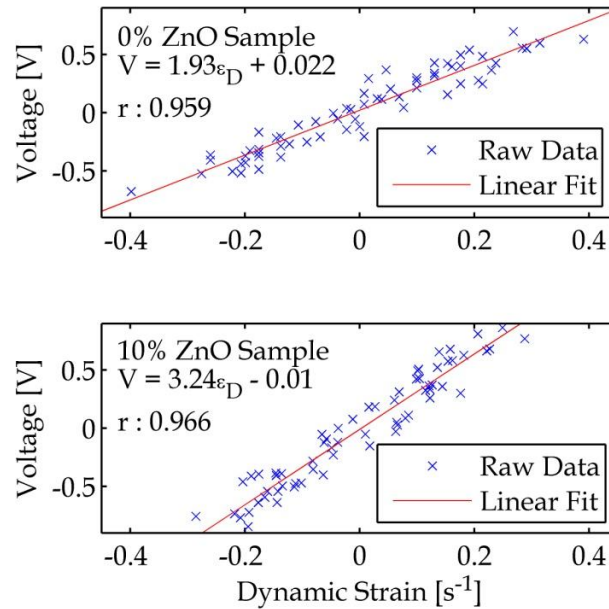

Fig. 11 The results from Fig. 10 have been processed and shown here. Thin film voltage response is plotted as a function of dynamic strain, and it is clear from these results that there is a linear relationship between voltage and dynamic strain, thereby indicating the potential for these films to be used as dynamic strain sensors. The top plot shows results for a 0 *wt.*% PVDF-TrFE/ZnO thin film, and the bottom corresponds to the case of a 10 *wt.*% nanocomposite

4. Conclusions

In this study, thin films of PVDF-TrFE embedded with ZnO nanoparticles (varying in *wt.%* from 0 to 20) have been fabricated using a combination of spin coating and annealing. Electrodes have been deposited across the films to give them functionality in the thickness direction. First, the films have been subjected to ferroelectric characterization tests for obtaining their piezoelectric and *D-E* hysteresis response; this has been achieved by applying high voltage AC signals to the films while measuring their electric polarization response using a Sawyer-Tower circuit. It has been found that higher concentrations of ZnO nanoparticles increase thin film remnant polarization and piezoelectricity. Next, the films have been poled using a high voltage DC electric field at 50 MV·m^{-1} for enabling permanent piezoelectricity. These films have been tested for their use as sensors using a hammer impact testing apparatus. The PVDF-TrFE/ZnO nanocomposites compare favorably with commercially poled PVDF-TrFE thin films. In addition, increasing ZnO weight content has also increased films' maximum generated voltages and performs better than the commercial specimens. Additional testing to characterize thin film voltage response with respect to impact energy and distance of the impact source has also been investigated. Finally, the as fabricated films have also been affixed onto cantilevered beam specimens subjected to free vibration testing. The results show that the films' voltage responses exhibit linear relationships with applied dynamic strains, thereby demonstrating their potential for use as dynamic strain sensors for SHM applications. Future research will involve more in-depth validation tests of these films, as well as exploring their use for actuation in a pitch-catch damage detection strategy.

Acknowledgments

References

Ahlborn, T.M., Shuchman, R., Sutter, L.L., Brooks, C.N., Harris, D.K., Burns, J.W., Endsley, K.A., Evans, D.C., Vaghefi, K. and Oats, R.C. (2010), *The state-of-the-practice of modern structural health monitoring for bridges: a comprehensive review*, Transportation Research Board.

Arlt, K. and Wegener, M. (2010), "Piezoelectric PZT / PVDF-copolymer 0-3 composites: aspects on film preparation and electrical poling", *IEEE T. Dielect. El. In.*, **17**(4), 1178-1184.

Barrager, S. and North, W. (2010), *Assessing and managing risks*, Paper presented at the IRGC Workshop.

Beeby, S.P., Tudor, M.J. and White, N.M. (2006), "Energy harvesting vibration sources for microsystems applications", *Meas. Sci. Technol.*, **17**(12), R175-R195.

Bharti, V., Kaura, T. and Nath, R. (1997), "Ferroelectric hysteresis in simultaneously stretched and corona-poled PVDF films", *IEEE T. Dielect. El. In.*, **4**(6), 738-741.

Defaÿ E. (Ed.) (2011) , *Integration of ferroelectric and piezoelectric thin films*, (Ed. Hoboken, NJ), John Wiley & Sons, Inc.

Devi, P.I. and Ramachandran, K. (2011), "Dielectric studies on hybridised PVDF-ZnO nanocomposites", *J. Exper. Nanosci.*, **6**(3), 281-293.

Dodds, J.S., Meyers, F.M. and Loh, K.J. (2012), "Piezoelectric characterization of PVDF-TrFE thin films enhanced with ZnO nanoparticles", *Sensors J. IEEE*, **12**(6), 1889 -1890.

Doebling, S.W., Farrar, C.R. and Prime, M.B. (1998), "A summary review of vibration-based damage identification methods", *Shock Vib.*, **30**(2), 91-105.

Farrar, C.R. and Worden, K. (2007), "An introduction to structural health monitoring", *Philos. T. R. Soc. A.*, **365**(1851), 303-315.

Gao, H., Guers, M.J., Rose, J.L., Zhao, G. and Kwan, C. (2006), *Ultrasonic guided wave annular array transducers for structural health monitoring*, Paper presented at the Quantitative Nondestructive Evaluation, Brunswick, ME.

Gaur, M.S. and Indolia, A.P. (2011), "Thermally stimulated dielectric properties of polyvinylidenefluoride-zinc oxide nanocomposites", *J. Therm. Anal. Calorim.*,**103**(3), 977-985.

Greeshma, T., Balaji, R., Nayak, M.M. and Jayakumar, S. (2009), "The influence of individual phases on piezoelectric coefficient of PZT-PVdF composites", *Ferroelectrics,* **393**(1), 88-93.

Gu, Y., Tong, L. and Tan, P. (2011), *Surface strain distribution method for delamination detection using piezoelectric actuators and sensors*. Paper presented at the Journal of Physics: Conference Series. Retrieved from http://stacks.iop.org/1742-6596/305/i=1/a=012077

Hasch, M. (2005), Beam collapse onto I-70 hurts 2. The tribune-review, from http://www.pittsburghlive.com /x/pittsburghtrib/s_408139.html.

Hilczer, B., Kulek, J., Markiewicz, E. and Szczesniak, L. (2000), "The method of matching resonance frequencies in coupled transmitter PVDF/TRFE diaphragms", *IEEE T. Dielect. El. In.*, **7**(4), 498-502.

Inman, D.J., Farmer, J. and Grisso, B.L. (2007), "Energy harvesting for autonomous sensing", *Key Eng. Mater.*, **347**, 405-410.

Kang, S.J., Park, Y.J., Sung, J., Jo, P.S., Park, C., Kim, J.K. and Cho, B.O. (2008), "Spin cast ferroelectric beta poly(vinylidene fluoride) thin films via rapid thermal annealing", *Appl. Phys. Lett.*, **92**(1), 012921-012923.

Kawai, H. (1969), "The piezoelectrcity of poly (vinylidene fluoride) ", *Jpn. J. Appl. Phys.*, **8**, 975-976.

Kersey, A.D. (1996), "A review of recent developments in fiber optic sensor technology", *Opt. Fiber Technol.*, **2**(3), 291-317.

La Saponara, V., Horsley, D.A. and Lestari, W. (2011), "Structural health monitoring of glass/epoxy composite plates using PZT and PMN-PT transducers", *J. Eng. Mater. Technol.*, **133**(1), 011011.

Loh, K. and Chang, D. (2010), "Zinc oxide nanoparticle-polymeric thin films for dynamic strain sensing", *J. Mater. Sci.*, **46**(1), 228-237.

Lynch, J.P. and Loh, K.J. (2006), "A summary review of wireless sensors and sensor networks for structural health monitoring", *Shock Vib.*, **38**(2), 91-128.

Mascarenas, D.L., Todd, M.D., Park, G. and Farrar, C.R. (2007), "Development of an impedance-based wireless sensor node for structural health monitoring", *Smart Mater. Struct.*, **16**(6), 2137-2145.

McKinney, J.E., Davis, G.T. and Broadhurst, M.G. (1980), "Plasma poling of poly(vinylidene fluoride): Piezo- and pyroelectric response", *J. Appl. Phys.*, **51**(3), 1676-1681.

Öğüt, E., Yördem, S., Menceloğlu, Y.Z. and Papila, M. (2007), *Poly(vinylidene fluoride)/Zinc Oxide Smart Composite Materials*, Paper presented at the Behavior and Mechanics of Multifunctional and Composite Materials.

Park, G., Sohn, H., Farrar, C.R. and Inman, D.J. (2003), "Overview of piezoelectric impedance-based health monitoring and path forward", *Shock Vib.*, **35**(6), 451-463.

Reid, R.L. (2010), "Damaged eyebar section replaced on San Francisco-Oakland Bay Bridge", *Civil Eng.*, **80**(4), 18-22.

Sodano, H.A., Inman, D.J. and Park, G. (2004), "A review of power harvesting from vibration using piezoelectric materials", *Shock Vib.*, **36**(3), 197-205.

Tu, Z.C. and Hu, X. (2006), "Elasticity and piezoelectricity of zinc oxide crystals, single layers, and possible single-walled nanotubes", *Phys. Rev. B.*, **74**(3), 035434.

Ulusoy, H.S., Feng, M.Q. and Fanning, P.J. (2011), "System identification of a building from multiple seismic records", *Earthq. Eng. Struct. D.,* **40**(6), 661-674.

Wang, Z.L. (2004), "Zinc oxide nanostructures: growth, properties and applications", *J. Phys. Condens. Matt.*, **16**(25), R829-R858.

Xu, S., Qin, Y., Xu, C., Wei, Y., Yang, R. and Wang, Z.L. (2010), "Self-powered nanowire devices", *Nature Nanotechnol.*, **5**, 366-373.

Zhang, Y., Baturin, I.S., Aulbach, E., Lupascu, D.C., Kholkin, A.L., Shur, V.Y. and Rodel, J. (2005), "Evolution of bias field and offset piezoelectric coefficient in bulk lead zirconate titanate with fatigue", *Appl. Phys. Lett.*, **86**(1), 012910.